(TRAIL) as a potential response marker for interferon-beta treatment in multiple sclerosis. Lancet 361: 2036–2043, 2003.
50) Lamhamedi-Cherradi S-E, Zheng S-J, Maguschak KA, Peschon J, Chen YH. Defective thymocyte apoptosis and accelerated autoimmune diseases in TRAIL$^{-/-}$ mice. Nature Immunol 4: 256–260, 2003.
51) Baranzini SE, Mousavi P, Rio J, Caillier SJ, Stillman A, Villoslada P, Wyatt MM, Comabella M, Greller LD, Somogyi R, Montalban X, Oksenberg JR. Transcription-based prediction of response to IFNβ using supervised computational methods. PLoS Biol 3: e2, 2005.

要　旨

多発性硬化症（multiple sclerosis; MS）発症は多数の遺伝因子と環境因子の複雑な相互作用により規定されている。そのため MS は臨床経過・病巣分布・治療反応性・病理学的所見の点から多様な病態（clinical heterogeneity）を呈する。遺伝子アレイ（DNA microarray, GeneChip）は基盤上に数万遺伝子が貼付けてあるチップである。遺伝子アレイによる MS 患者末梢血リンパ球や脳組織の網羅的遺伝子発現解析は，MS の分子遺伝学的発症機序解明に威力を発揮する。特に遺伝子アレイ解析により従来の研究方法では予期しなかった遺伝子群の MS 病態における重要な役割を発見したり，インターフェロン応答遺伝子群（IFN-responsive gene; IRG）を同定することにより治療有効性や副作用を事前に予知することが可能になりつつある。最近我々は階層的クラスター解析（hierarchical clustering analysis）により，MS が T 細胞の遺伝子発現プロフィールに基づき 4 群に分類され，各群は疾患活動性・病変分布・インターフェロン（IFNβ）治療反応性と密接な対応を認めることを発見した。遺伝子アレイ解析は MS のテーラーメイド医療（personalized medicine）樹立に道を開くと思われる。

キーワード：遺伝子発現プロフィール，DNA マイクロアレイ，多発性硬化症，テーラーメイド医療

ELSEVIER

Journal of Neuroscience Methods 152 (2006) 278–288

JOURNAL OF NEUROSCIENCE METHODS

www.elsevier.com/locate/jneumeth

Rapid identification of 14-3-3-binding proteins by protein microarray analysis

Jun-ichi Satoh [a,b,*], Yusuke Nanri [a], Takashi Yamamura [a]

[a] *Department of Immunology, National Institute of Neuroscience, NCNP, 4-1-1 Ogawahigashi, Kodaira, Tokyo 187-8502, Japan*
[b] *Department of Bioinformatics and Neuroinformatics, Meiji Pharmaceutical University, 2-522-1 Noshio, Kiyose, Tokyo 204-8588, Japan*

Received 8 June 2005; received in revised form 19 September 2005; accepted 26 September 2005

Abstract

The 14-3-3 protein family consists of acidic 30-kDa proteins composed of seven isoforms in mammalian cells, expressed abundantly in neurons and glial cells of the central nervous system (CNS). The 14-3-3 isoforms form a dimer that acts as a molecular adaptor interacting with key signaling components involved in cell proliferation, transformation, and apoptosis. Until present, more than 300 proteins have been identified as 14-3-3-binding partners, although most of previous studies focused on a limited range of 14-3-3-interacting proteins. Here, we studied a comprehensive profile of 14-3-3-binding proteins by analyzing a high-density protein microarray using recombinant human 14-3-3 epsilon protein as a probe. Among 1752 proteins immobilized on the microarray, 20 were identified as 14-3-3 interactors, most of which were previously unreported 14-3-3-binding partners. However, 11 known 14-3-3-binding proteins, including keratin 18 (KRT18) and mitogen-activated protein kinase-activated protein kinase 2 (MAPKAPK2), were not identified as a 14-3-3-binding protein. The specific binding to 14-3-3 of EAP30 subunit of ELL complex (EAP30), dead box polypeptide 54 (DDX54), and src homology three (SH3) and cysteine rich domain (STAC) was verified by immunoprecipitation analysis of the recombinant proteins expressed in HEK293 cells. These results suggest that protein microarray is a powerful tool for rapid and comprehensive profiling of 14-3-3-binding proteins.

Keywords: 14-3-3-Binding protein; Immunoprecipitation; Protein microarray; Protein–protein interaction; STAC

1. Introduction

The 14-3-3 protein family consists of evolutionarily conserved, acidic 30-kDa proteins composed of seven isoforms named β, γ, ε, ζ, η, θ, and σ in mammalian cells. A homodimeric or heterodimeric complex composed of the same or distinct isoforms constitutes a large cup-like structure possessing an amphipathic groove with two ligand-binding capacity (Fu et al., 2000; van Hemert et al., 2001). The dimeric complex acts as a molecular adaptor that interacts with key signaling molecules involved in cell differentiation, proliferation, transformation, and apoptosis. It regulates the function of target proteins by restricting their subcellular location, bridging them to modulate catalytic activity, and protecting them from dephosphorylation or proteolysis (Dougherty and Morrison, 2004; MacKintosh, 2004). Although 14-3-3 is widely distributed in neural and non-neural tissues, it is expressed most abundantly in neurons in the central nervous system (CNS), where it represents 1% of total cytosolic proteins (Berg et al., 2002). Aberrant expression and impaired function of 14-3-3 in the CNS are associated with pathogenetic mechanisms of Creutzfeldt–Jacob disease, Alzheimer disease, Parkinson disease, spinocerebellar ataxia, amyotrophic lateral sclerosis, and multiple sclerosis (Chen et al., 2003; Kawamoto et al., 2002; Layfield et al., 1996; Malaspina et al., 2000; Satoh et al., 2004; Zerr et al., 1998).

In general, the 14-3-3 protein interacts with phosphoserine-containing motifs of the ligands such as RSXpSXP (mode I) and RXXXpSXP (mode II) in a sequence-specific manner (Dougherty and Morrison, 2004; MacKintosh, 2004). Previously, more than 300 proteins have been identified as being 14-3-3-binding partners. They include key signaling components, such as Raf-1 kinase, Bcl-2 antagonist of cell death (BAD), protein kinase C (PKC), phophatidylinositol 3-kinase (PI3K), and cdc25 phosphatase (Fu et al., 2000; van Hemert et al., 2001). Binding of 14-3-3 to Raf-1 is indispensable for its kinase activity in the Ras-MAPK signaling pathway, and the interaction of 14-3-3 with BAD, when phosphorylated by

* Corresponding author. Tel.: +81 42 341 2711; fax: +81 42 346 1753.
E-mail address: satoj@ncnp.go.jp (J.-i. Satoh).

0165-0270/$ – see front matter © 2005 Elsevier B.V. All rights reserved.
doi:10.1016/j.jneumeth.2005.09.015

a serine/threonine kinase Akt, inhibits apoptosis. Recent studies indicate that the 14-3-3 protein could interact with a set of target proteins in a phosphorylation-independent manner (Dai and Murakami, 2003; Henriksson et al., 2002; Zhai et al., 2001). Increasing knowledge of interactions between 14-3-3 and interacting molecules would help us to understand the biological function and pathological implication of the 14-3-3 protein networks.

The yeast two-hybrid (Y2H) system is a powerful approach to identify novel protein–protein interactions. However, Y2H screening requires a lot of time and effort, and is often criticized for detecting the interactions unrelated to the physiological setting and obtaining high rates of false positive interactors caused by spontaneous activation of reporter genes and self-activating bait proteins (Vidalain et al., 2004; Zhang et al., 2004). Affinity purification coupled with mass spectrometry (APMS) is an alternative approach to identify the components of protein complexes on a large scale. This approach has been taken to identify a wide variety of 14-3-3-interacting proteins involved in cell proliferation, metabolism, and survival (Benzinger et al., 2005; Jin et al., 2004; Meek et al., 2004; Pozuelo Rubio et al., 2004). Although the APMS procedure detects binding partners of physiological significance, it is laborious and has a difficulty in detecting transmembrane proteins and loosely associated components that might be lost during purification (von Mering et al., 2002). Recently, protein microarray technology has been established for rapid, systematic, and less expensive screening of thousands of protein–protein, protein–lipid, and protein–nucleic acid interactions in a high-throughput fashion. This approach has important applications in the areas not only of basic biological research but also of drug discovery research, including identification of the substrates of protein kinases and the protein targets of small molecules (Chan et al., 2004; MacBeath and Schreiber, 2000; Michaud et al., 2003; Zhu et al., 2001).

The present study was designed for the first time to identify a comprehensive profile of human 14-3-3-binding proteins by analyzing a high-density protein microarray.

2. Materials and methods

2.1. Preparation of a probe for microarray analysis

Human embryonic kidney cells HEK293 whose genome was modified for the Flp-In system (Flp-In 293) were obtained from Invitrogen, Carlsbad, CA. Flp-In 293 cells contain a single Flp recombination target (FRT) site targeted for the site-specific recombination, integrated in a transcriptionally active locus of the genome, where it stably expresses the *lacZ*-Zeocin fusion gene driven from the pFRT/*lac*Zeo plasmid under the control of SV40 early promoter. Flp-In 293 cells were maintained in Dulbecco's modified Eagle's medium (DMEM) supplemented with 10% fetal bovine serum (FBS), 100 U/ml of penicillin, and 100 μg/ml of streptomycin (feeding medium) with inclusion of 100 μg/ml of Zeocin (Invitrogen) as described previously (Satoh and Yamamura, 2004).

To prepare the probe for protein microarray analysis, the open reading frame (ORF) of the human 14-3-3ε gene (YWHAE) was amplified from cDNA of NTera2-N cells (Satoh and Kuroda, 2000) by PCR using PfuTurbo DNA polymerase (Stratagene, La Jolla, CA, USA) and the primer sets listed in Table 1. The PCR product was then cloned into a mammalian expression vector pSecTag/FRT/V5-His TOPO (Invitrogen) to produce a fusion protein with a C-terminal V5 (GKPIPNPLLGLDST) tag, a C-terminal polyhistidine (6 × His) tag, and an N-terminal Ig κ-chain secretion signal. This vector, together with the Flp recombinase expression vector pOG44 (Invitrogen), was transfected in Flp-In 293 cells by Lipofectamine 2000 reagent (Invitrogen). A stable cell line was established after incubating the transfected cells for approximately 1 month in the feeding medium with inclusion of 100 μg/ml of Hygromycin B (Invitrogen). It was named 293 eV5. The recombinant protein was secreted into the culture medium of 293 eV5 cells after the Ig κ-chain secretion signal sequence was processed by an endogenous signal peptidase-mediated cleavage.

To purify the recombinant 14-3-3ε protein, the culture supernatant of 293 eV5 cells incubated for 48 h in the serum-free DMEM/F-12 medium was harvested and concentrated at an 1/40 volume by centrifugation on an Amicon Ultra-15 filter (Millipore, Bedford, MA). It was then purified by the HIS-select spin column (Sigma, St. Louis, MO) and concentrated at an 1/10 volume by centrifugation on a Centricon-10 filter (Millipore). The protein concentration was determined by a Bradford assay kit (BioRad, Hercules, CA). The purity and specificity of the probe were verified by Western blot analysis using mouse monoclonal anti-V5 antibody (Invitrogen) and rabbit polyclonal antibody specific for the 14-3-3ε isoform (IBL, Gumma, Japan).

2.2. Protein microarray analysis

ProtoArray human protein microarray (v1.0) commercially available from Invitrogen was utilized in the present study. It contains 1752 human proteins of various functional classes spotted in duplicate on a nitrocellulose-coated glass slide. To prepare target proteins immobilized on the microarray, an N-terminal glutathione-*S* transferase (GST)-6× His fusion protein derived from the genes selected from the human ultimate ORF clone collection (Invitrogen) was expressed in Sf9 insect cells by using the baculovirus expression system (Invitrogen). Either the full-length or the partial fragment of recombinant proteins, was purified under native conditions by glutathione affinity chromatography in the presence of protease inhibitors, then processed for spotting on the slides. The proteins were printed in an arrangement composed of 4 × 12 subarrays equally spaced in vertical and horizontal directions (Fig. 1a). Each subarray included 16 × 16 spots, composed of 48 control spots (C), 80 human proteins (H), and 128 blanks (B) (Fig. 1c). The control proteins (C) were composed of 14 positive control spots and 34 negative control spots. The former includes four spots of an Alexa Fluor 647-labeled antibody (rows 1, 8; columns 1, 2), six spots of a concentration gradient of a biotinlyated anti-mouse antibody with a capacity to bind to mouse monoclonal anti-V5 antibody conjugated with Alexa Fluor 647 (row 8; columns 3–8), and four spots of a concentration gradient of V5 protein (row 8; columns 13–16). The latter includes six spots of

Table 1
Primers utilized for PCR-based cloning and site-directed mutagenesis

Genes	Proteins (amino acid residues)	GenBank accession no.	Sense primers	Antisense primers	Cloning vector
YWHAE	14-3-3ε Isoform (2-255)	NM_006761	5′gatgatcgaggaggatctggtgtac3′	5′ctgattttcgtcttccacgtcctg3′	pSecTag/FRT/V5-His TOPO
EAP30	EAP30 subunit of ELL complex (2-258)	NM_007241	5′caccgccgcgggtggaggctggcc3′	5′tcagggcgaggcttctctggcctc3′	pcDNA4/HisMax-TOPO
DDX54	Dead box polypeptide 54 (2-881)	NM_024072	5′gcggccgacaaggcccgggcggct3′	5′tcacatcctcttccgcatcttgcc3′	pcDNA4/HisMax-TOPO
STAC	src homology three and cysteine rich domain (2-402, full length)	NM_003149	5′atccctccgagcagcccccgcgag3′	5′tcagatgtttctagtacatccaag3′	pcDNA4/HisMax-TOPO
STAC	src homology three and cysteine rich domain (2-402 with S172A; SMT)	NM_003149	5′gttcggcgttactacgcctccccctt-gctcattc3′	5′gaatgagcaagggggaggcgtagtaa-cgccgaaac3′	pcDNA4/HisMax-TOPO modified by site-directed mutagenesis
STAC	src homology three and cysteine rich domain (2-402 with S172A and S173A; DMT)	NM_003149	5′cggcgttactacgccgccccctt-gctcattcat3′	5′atgaatgagcaagggggcggcgt-agtaacgccg3′	pcDNA4/HisMax-TOPO modified by site-directed mutagenesis
STAC	src homology three and cysteine rich domain (2-233, N-terminal half; NTF)	NM_003149	5′atccctcgagcagcccccgcgag3′	5′tcaaagatctgaagtagaggttct3′	pcDNA4/HisMax-TOPO
STAC	src homology three and cysteine rich domain (234-402, C-terminal half; CTF)	NM_003149	5′gtggaggttcctgaggaagccaat3′	5′tcagccacctggatgcagaccagc3′	pcDNA4/HisMax-TOPO
STAC	src homology three and cysteine rich domain (2-164, truncated form A; TR-A)	NM_003149	5′atccctcgagcagcccccgcgag3′	5′tcatggcagcttgcccatgcaccg3′	pcDNA4/HisMax-TOPO
STAC	src homology three and cysteine rich domain (2-105, truncated form B; TR-B)	NM_003149	5′atccctcgagcagcccccgcgag3′	5′tcagccacctggatgcagaccagc3′	pcDNA4/HisMax-TOPO

The PCR product was cloned into a vector pSecTag/FRT/V5-His TOPO to express a fusion protein with a V5 tag or into a vector pcDNA4/HisMax-TOPO to express a fusion protein with a Xpress tag in HEK293 cells.

a concentration gradient of bovine serum albumin (BSA) (row 1; columns 3–8), four spots of a concentration gradient of a rabbit anti-GST antibody (row 1; columns 9–12), four spots of a concentration gradient of calmodulin (row 1; columns 13–16), 16 spots of a concentration gradient of GST (row 2; columns 1–16), two spots of buffer only (row 8; columns 9,10), and two spots of an anti-biotin antibody (row 8; columns 11,12). The complete list of 1752 target proteins immobilized on the microarary is shown in Supplementary Table 1 online.

Non-specific binding was blocked by incubating the microarray for 90 min in the PBST blocking buffer composed of 1% BSA and 0.1% Tween 20 in phosphate-buffered saline (PBS). Then, it was incubated for 30 min at 4 °C with the probe described above at a concentration of 50 μg/ml in the probing buffer composed of 1% BSA, 5 mM $MgCl_2$, 0.5 mM dithiothreitol (DTT), 0.05% Triton X-100, and 5% glycerol in PBS. The array was washed three times with the probing buffer, followed by incubation for 30 min at 4 °C with mouse monoclonal anti-V5 antibody conjugated with Alexa Fluor 647 (Invitrogen) at a concentration of 260 ng/ml in the probing buffer. The array was washed three times with the probing buffer, and then scanned by the GenePix 4200A scanner (Axon Instruments, Union City, CA) at a wavelength of 635 nm. The data were analyzed by using the ProtoArray Prospector software v2.0 (Invitrogen) following acquisition of the microarray lot-specific information online, including inter-lot variations in protein concentrations (http://www.invitrogen.com/protoarray). According to the default setting of the software, the spots showing the background-subtracted signal intensity value greater than the median plus three standard deviations of all the fluorescence intensities were considered as having a significant binding. The Z-score, an indicator for statistical evaluation of binding specificity, was calculated as the background-subtracted signal intensity value of the target protein minus the average of the background-subtracted signal intensity value from the negative control distribution, divided by the standard deviation of the negative control distribution. All the procedure described above could be accomplished within 5 h. The 14-3-3-binding consensus motif mode I (RSXpSXP) sequence located in target proteins was surveyed by the Scansite Motif Scanner, which assesses the probability of a site matching the candidate motif under high, medium, or low stringent conditions (Obenauer et al., 2003). The information on known 14-3-3 interactors was obtained from Biomolecular Interaction Network Database (BIND; http://www.bind.ca) and PubMed database search.

2.3. Transient expression of 14-3-3-binding proteins in HEK293 cells

To verify the results of microarray analysis, the ORF of the genes encoding EAP30 subunit of ELL complex (EAP30), dead box polypeptide 54 (DDX54), and src homology three (SH3) and cysteine rich domain (STAC) were amplified by PCR using PfuTurbo DNA polymerase and the primer sets listed in Table 1. They were then cloned into a mammalian expression vector pcDNA4/HisMax-TOPO (Invitrogen) to produce a fusion protein with an N-terminal Xpress tag. To express the STAC mutant

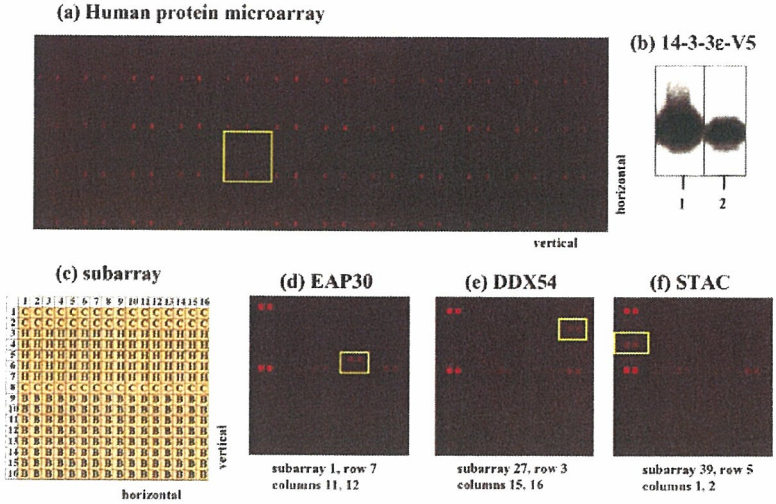

Fig. 1. Protein microarray analysis. (a) Human protein microarray. The microarray contains 1752 distinct human proteins of various functional classes spotted in duplicate on a nitrocellulose-coated glass slide. They are printed in an arrangement of 4 × 12 subarrays equally spaced in vertical and horizontal directions. A representative subarray is indicated by an enclosed yellow line. (b) Recombinant human 14-3-3ε protein tagged with V5. One microgram of the protein was processed for Western blot analysis using anti-V5 antibody (lane 1) or anti-14-3-3ε antibody (lane 2). (c) Layout of the subarray. Each subarray includes 16 × 16 spots composed of 48 control spots (C), 80 human proteins (H), and 128 blanks (B). The positive control spots include an Alexa Fluor 647-labeled antibody (rows 1, 8; columns 1, 2; strong signals), a concentration gradient of a biotinylated anti-mouse antibody with a capacity to bind to mouse monoclonal anti-V5 antibody conjugated with Alexa Fluor 647 (row 8; columns 3–8; signals visible on the higher concentration), and a concentration gradient of V5 protein (row 8; columns 13–16; signals visible on the higher concentration). (d) EAP30. (e) DDX54. (f) STAC. The three proteins indicated by an enclosed yellow line located on different subarrays (d–f) represent an example identified as showing significant binding to the probe.

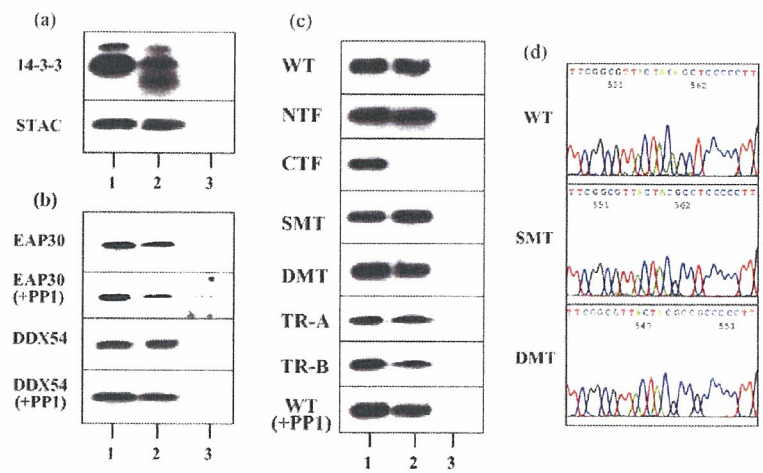

Fig. 2. Immunoprecipitation analysis of 14-3-3-binding proteins. (a) Binding of STAC to 14-3-3. Total protein extract of HEK293 cells expressing Xpress-tagged recombinant STAC was processed for immunoprecipitation (IP) with rabbit polyclonal antibody reacting with all 14-3-3 isoforms (K-19) or with normal rabbit IgG. The immunoprecipitates were then processed for Western blot analysis using mouse monoclonal antibody reacting with all 14-3-3 isoforms (H-8) (upper panel) or mouse monoclonal anti-Xpress antibody (lower panel). Lanes (1–3) represent (1) the input control, and IP with (2) K-19 and (3) normal rabbit IgG. (b) Binding of EAP30 and DDX54 to 14-3-3. Total protein of HEK293 cells expressing Xpress-tagged recombinant EAP30 or DDX54 extracted by using the lysis buffer with inclusion of phosphatase inhibitors or with inclusion of protein phosphatase-1 (PP1) instead of phosphatase inhibitors (+PP1) was processed for IP with K-19 or with normal rabbit IgG. The immunoprecipitates were then processed for Western blot analysis using anti-Xpress antibody. Lanes (1–3) represent (1) the input control, and IP with (2) K-19 and (3) normal rabbit IgG. (c) Binding of mutant and truncated STAC to 14-3-3. Total protein was extracted from HEK293 cells expressing a panel of Xpress-tagged recombinant STAC proteins. They include the full-length wild-type (WT) STAC, the N-terminal half (NTF), the C-terminal half (CTF), the S172A mutant (SMT), the S172A and S173A double mutant (DMT), the truncated form lacking the 14-3-3-binding consensus motif RYYSSP (TR-A), the truncated form lacking the cysteine-rich domain (CRD) (TR-B), and WT STAC isolated by using the lysis buffer with inclusion of PP1 instead of phosphatase inhibitors (WT + PP1). Primers utilized for PCR-based cloning and site-directed mutagenesis are listed in Table 1. The lysate was processed for IP with K-19 or with normal rabbit IgG. The immunoprecipitates were then processed for Western blot analysis using anti-Xpress antibody. Lanes (1–3) represent (1) the input control, and IP with (2) K-19 and (3) normal rabbit IgG. (d) The sequence of the 14-3-3-binding consensus motif located in amino acid residues 169-174 in expression vectors of STAC. The panels indicate WT (nucleotide sequence CGT-TAC-TAC-AGC-TCC-CCC: the corresponding amino acid sequence RYYSSP), SMT (CGT-TAC-TAC-GCC-TCC-CCC: RYYASP), and DMT (CGT-TAC-TAC-GCC-GCC-CCC: RYYAAP).

with a single amino acid substitution S172A (the single mutant; SMT) or with double amino acid substitutions S172A and S173A (the double mutant; DMT), the pcDNA4/HisMax-TOPO vector containing the wild-type (WT) STAC gene was modified by consecutive site-directed mutagenesis using QuikChange II site-directed mutagenesis kit (Stratagene) and the primer sets listed in Table 1. The mutations introduced in the vector were verified by sequencing analysis (Fig. 2d). All these vectors were transfected in HEK293 cells by Lipofectamine 2000 reagent.

2.4. Immunoprecipitation analysis

To prepare total protein extract, the cells were homogenized and incubated at room temperature for 30 min in M-PER lysis buffer (Pierce, Rockford, IL) supplemented with a cocktail of protease inhibitors (Sigma), with inclusion of phosphatase inhibitors (Sigma) to maintain the protein phosphorylation status or with inclusion of recombinant protein phosphatase-1 (PP1) catalytic subunit α-isoform (5 U/ml; Sigma) instead of phosphatase inhibitors to induce the protein dephosphorylation reaction (Ichimura et al., 2005), followed by centrifugation at 12,000 rpm at 4 °C for 20 min. After preclearance, the supernatant was incubated at 4 °C for 3 h with 30 μg/ml rabbit polyclonal anti-14-3-3 protein antibody (K19)-conjugated agarose (Santa Cruz Biotechnology, Santa Cruz, CA) or the same amount of normal rabbit IgG-conjugated agarose (Santa Cruz Biotechnology). After several washes, the immunoprecipitates were processed for Western blot analysis using mouse monoclonal anti-14-3-3 protein antibody (H-8, Santa Cruz Biotechnology) and mouse monoclonal anti-Xpress antibody (Invitrogen). K-19 and H-8 antibodies recognize all 14-3-3 isoforms. The specific reaction was visualized using a chemiluminescent substrate (Pierce).

3. Results

3.1. Protein microarray analysis identified 20 distinct 14-3-3-binding partners

To analyze a high-density human protein microarray, the recombinant 14-3-3ε protein tagged with V5 was purified form the supernatant of 293 eV5 cells secreting the recombinant protein in the culture medium. Western blot analysis verified the purity and specificity of the probe (Fig. 1b). Among 1752 proteins on the microarray, 20 were identified as the proteins showing significant binding to the probe (Table 2). All of these were previously unreported 14-3-3-binding partners by the BIND search. Seven were hypothetical clones of uncharacterized function, derived from the mammalian genome collection (MGC) or the full-length long Japan (FLJ). Thirteen annotated proteins included EAP30 subunit of ELL complex (EAP30) (Fig. 1d), lymphocyte cytosolic protein 2 (LCP2), methionine aminopeptidase 2 (METAP2), melanoma antigen family B, 4 (MAGEB4), chondroitin 4 sulfotransferase 11 (CHST11), nuclear interacting partner of anaplastic lymphoma kinase (ZC3HC1), minichromosome maintenance deficient 10 (MCM10), DEAD box polypeptide 54 (DDX54) (Fig. 1e), heterogeneous nuclear ribonucleoprotein C (HNPRC), fibroblast growth factor 12 (FGF12), glutathione *S*-transferase M3 (GSTM3), src homology three (SH3) and cysteine rich domain (STAC) (Fig. 1f), and ATPase, H+ transporting, lysosomal, 21 kDa, V0 subunit C″ (ATP6V0B). The 14-3-3-binding consensus motif mode I (RSX*p*SXP) was found only in STAC (*pS*172) and HNRPC (*pS*125) by the Scansite Motif Scanner search under the high stringent condition, while 15 of 20 proteins have one or several motifs when a query with the medium or low stringency was performed (Table 2).

3.2. Immunoprecipitation analysis validated the specific binding to 14-3-3

EAP30, DDX54, and STAC were selected to verify the results of microarray analysis, in view of their higher Z-scores. The recombinant proteins were expressed in HEK293 cells, which constitutively express a substantial amount of endogenous 14-3-3 protein. Total protein was extracted by using the lysis buffer with inclusion of phosphatase inhibitors to maintain the protein phosphorylation status or with inclusion of recombinant protein phosphatase-1 (PP1) instead of phosphatase inhibitors to induce the protein dephosphorylation reaction, followed by processing for immunoprecipitation (IP) with rabbit polyclonal antibody reacting with all 14-3-3 isoforms (K-19) or with normal rabbit IgG. K19 coimmunoprecipitated 14-3-3 and STAC from the lysate of HEK293 cells expressing the recombinant STAC protein, whereas normal rabbit IgG did not pull down these proteins (Fig. 2a). K-19 immunoprecipitated EAP30 and DDX54 from the lysate of HEK293 cells expressing the recombinant EAP30 or DDX54 protein, respectively, under both phosphorylated and dephosphorylated conditions (Fig. 2b). These results indicate that EAP30, DDX54, and STAC could interact with the endogenous 14-3-3 protein in HEK293 cells where the corresponding recombinant proteins were expressed.

STAC has the highly stringent 14-3-3-binding consensus motif RYYSSP in amino acid residues 169-174 (*pS*172), as suggested by the Scansite Motif Scanner (Table 2). Therefore, a possible involvement of this motif in binding to 14-3-3 was investigated by IP analysis of a series of mutant and truncated STAC proteins (Table 1). K-19 immunoprecipitated the full-length wild-type (WT) STAC comprised of amino acid residues 2-402 (Fig. 2a and c). K-19 also pulled down the S172A mutant (SMT), and the S172A and S173A double mutant (DMT), and the N-terminal half (NTF; amino acid residues 2-233) from the lysate of HEK293 cells expressing the corresponding recombinant proteins (Fig. 2c). In contrast, K-19 did not pull down the C-terminal half (CTF; amino acid residues 234-402) (Fig. 2c). These observations indicate that the RYYSSP motif is not essential for binding of STAC to 14-3-3. This was confirmed by the observations that K-19 immunoprecipitated the truncated form lacking the RYYSSP sequence (TR-A; amino acid residues 2-164) and the shortest form lacking both the RYYSSP sequence and the cysteine-rich domain (CRD) (TR-B; amino acid residues 2-105) from the lysate of HEK293 cells expressing the corresponding recombinant proteins (Fig. 2c). Finally, the full-length WT STAC interacted with 14-3-3 under the dephosphorylated condition (Fig. 2c). These observations indicate that the

Table 2
Twenty 14-3-3-binding proteins identified by protein microarray analysis

No.	Symbol	Database ID	Protein name	Putative biological function	14-3-3-binding consensus motif mode I	Stringency level of the binding motif	Subarray	Row	Column	Z-score
1	EAP30	NM_007241	EAP30 subunit of ELL complex	a 30-kDa component of the ELL complex that confers derepression of transcription by RNA polymerase II	No sites	NA	1	7	11	22.8593
									12	24.60829
2	FLJ10415	NM_018089	Hypothetical protein, cDNA clone MGC:969	Unknown	S258: ARGGPSHSAGANLRR	Low	5	4	11	4.16265
					S405: SPKQGSGSEGEDGFQ	Low			12	4.35203
					S525: PADPRVLSLLSAPLG	Low				
					S690: VNTRRCWSCGASLQG	Low				
3	LOC57228	NM_020467	Hypothetical protein	Unknown	S28: AARKRNISSNDSQAP	Low	5	6	9	16.84741
									10	17.1519
4	MGC17403	NM_152634	Hypothetical protein	Unknown	T274: KQLRASYTESCIQEH	Low	11	3	1	4.04754
									2	4.08838
5	LCP2	NM_005565	Lymphocyte cytosolic protein 2	A 72-kDa protein (SLP76) that associates with the Grb2 adaptor protein, provides a substrate of the ZAP-70 protein tyrosine kinase, and plays a role in promoting T cell development and activation	S297: TTERHERSSPLPGKK	Low	13	5	11	4.47457
					S376: SSFPQSASLPPYFSQ	Low			12	4.46343
					T456: DSSKKTTTNPYVLMV	Low				
6	METAP2	NM_006838	Methionine aminopeptidase 2	A 67-kDa protein that interacts with eukaryotic initiation factor-2 (eIF-2) and regulates protein synthesis	T113: KRGPKVQTDPPSVPI	Low	15	6	11	3.54252
					S152: TAAWRTTSEEKKALD	Low			12	3.31601
7	MAGEB4	NM_002367	Melanoma antigen family B, 4	A member of the MAGEB family expressed in testis whose function remains unknown	T18: AREKRQRTRGQTQDL	Medium	18	3	7	9.50614
					T194: GNQSSAWTLPRNGLL	Low			8	9.30562
					S339: SAYSRATSSSSSQPM	Low				
8	CHST11	NM_018413	Chondroitin 4 sulfotransferase 11	A member of HNK-1ST family GalNAc 4-O-sulfotransferase that plays a role in chondroitin sulfate and dermatan sulfate biosynthesis	S93: TDTCRANSATSRKRR	Medium	20	5	3	3.97327
					S56: DICCRKGSRSPLQEL	Low			4	3.92871
					S194: EPFERLVSAYRNKFT	Low				
9	ZC3HC1	NM_016478	Nuclear interacting partner of anaplastic lymphoma kinase (ALK)	A 60-kDa protein that interacts with ALK and plays an antiapoptotic role in nucleophosmin-ALK signaling events	No sites	NA	23	3	3	3.33458
									4	3.55366

Table 2 (*Continued*)

No.	Symbol	Database ID	Protein name	Putative biological function	14-3-3-binding consensus motif mode I	Stringency level of the binding motif	Subarray	Row	Column	Z-score
10	MCM10	NM_018518	Minichromosome maintenance deficient 10	A key component of the pre-replication complex (pre-RC) that is essential for the initiation of DNA replication	S90: AQPPRTGSEFPRLEG	Medium	25	3	13	4.26291
					S35: KPAIKSISASALLKQ	Low			14	4.12552
					S55: LEMRRRKSEEIQKRF	Low				
					S302: PCGNRSISLDRLPNK	Low				
					T329: DGMLKEKTGPKIGGE	Low				
11	DDX54	NM_024072	DEAD (Asp-Glu-Ala-Asp) box polypeptide 54	A 97-kDa RNA helicase (DP97) that interacts with estrogen receptor (ER) and represses the transcription of ER-regulated genes	T95: EDKKKIKTESGRYIS	Low	27	3	15	9.2425
					S102: TESGRYISSSYKRDL	Low			16	9.10882
12	HNPRC	NM_004500	Heterogeneous nuclear ribonucleoprotein C	A member of heterogeneous nuclear ribonucleoproteins (hnRNPs) involved in pre-mRNA processing, mRNA metabolism and transport	S125: DYYDRMYSYPARVPP	High	28	6	9	4.81248
					S158: NTSRRGKSGFNSKSG	Low			10	5.18382
					S170: KSGQRGSSKSGKLKG	Low				
					S240: ETNVKMESEGGADDS	Low				
13	LOC137781	BC032347	Hypothetical gene, cDNA clone MGC:40429	Unknown	No sites	NA	30	5	11	3.56109
									12	3.47568
14	LOC92345	NM_138386	Hypothetical protein	Unknown	S339: QGRKKLKSEFNEPGE	Low	32	5	13	3.55366
					T374: GYRNREFTRGFSRAR	Low			14	3.73933
					S467: PLLNLPYSLPPPPPP	Low				
15	FGF12	NM_004113	Fibroblast growth factor 12, transcript variant 2	A member of the FGF family that plays a role in nervous system development and function	S150: VCMYREQSLHEIGEK	Low	34	6	5	5.73339
					S165: QGRSRKSSGTPTMNG	Low			6	5.75567
16	GSTM3	NM_000849	Glutathione *S*-transferase M3 (brain)	A cytoplasmic glutathione *S*-transferase of the mu class that plays a role in detoxification of carcinogens, therapeutic drugs, environmental toxins, and products of oxidative stress	S64: GIKLRSFSV	Low	38	5	15	7.82029
									16	7.70889
17	STAC	NM_003149	src homology three (SH3) and cysteine rich domain	A 47-kDa protein with a SH3 and a cysteine-rich domain that plays a role in the neuron-specific signal transduction pathway	S172: KGFRRYYSSPLLIHE	High	39	5	1	16.63575
					S56: TKSLRSKSADNFFQR	Medium			2	16.64318
					S255: DLRKRSNSVFTYPEN	Medium				
					S46: QKLKRSLSFKTKSLR	Low				
					S51: SLSFKTKSLRSKSAD	Low				
					S66: NFFQRTNSEDMKLQA	Low				
					S253: GYDLRKRSNSVFTYP	Low				

18	FLJ10156	NM_019013	Hypothetical protein, cDNA clone MGC:961	Unknown	S16: GTSVRRRSLQHQEQL	Low	41	3	7		7.31156
					T190: FRSPYSSTEPLCSPS	Low			8		6.94023
19	ATP6V0B	NM_004047	ATPase, H+ transporting, lysosomal, 21 kD, V0 subunit C″	A 23-kDa component of vacuolar ATPase that mediates acidification of intracellular organelles	No sites	NA	43	7	3		3.3123
									4		3.60565
20	FLJ25758	NM_001011541	Hypothetical protein, clone MGC:33355	Unknown	No sites	NA	48	7	7		4.18864
									8		4.18122

Among 1752 proteins on the microarray, 20 were identified as showing a significant interaction, based on the signal intensity value exceeding the median plus three standard deviations of all the fluorescence intensities by analyzing with ProtoArray Prospector software. They are listed with the 14-3-3-binding consensus motif (putative phosphoserine and phosphothreonine indicated by underline) and its stringency level by the Scansite Motif Scanner, the position on the array, and the Z-score calculated as described in Section 2. Abbreviations: FLJ, the full-length long Japan; MCG, mammalian gene collection; NA, not available.

14-3-3-interacting domain is located in the N-terminal segment spanning amino acid residues 2-105 of STAC, and the interaction is independent of serine/threonine-phosphorylation of the binding domain of STAC.

4. Discussion

The present study was designed to rapidly and systematically identify 14-3-3-binding proteins by analyzing a high-density protein microarray. The array included 1752 proteins derived from multiple gene families of biological importance, including cell-signaling proteins, kinases, membrane-associated proteins, and metabolic proteins. In general, protein microarray has its own limitations associated with the expression and purification of a wide variety of target proteins. In the microarray we utilized, the target proteins were expressed in a baculovirus expression system, purified under native conditions, and spotted on the slides to ensure the preservation of native structure, posttranslational modifications, including glycosylation and serine phophorylation (Culleré et al., 1998; Tennagels et al., 1999), and proper functionality. Immunolabeling of the array with anti-phosphotyrosine (pTyr) antibody indicated that approximately 10–20% of the proteins on the array are phosphorylated (the unpublished data of Invitrogen Technical Service). When this microarray was utilized for kinase substrate identification, most of known kinases immobilized on the array are enzymatically active with the capacity of some degree of autophosphorylation, suggesting that they are certainly phosphorylated on tyrosine, serine, and threonine residues (see the Protoarray application note on http://www.invitrogen.com/protoarray). However, we could not currently validate the precise levels of phosphorylation of individual proteins, because of a lack of anti-phosphoserine (pSer) and anti-phosphothreonine (pThr) antibodies suitable for detection of pSer and pThr residues of the proteins on glass slide.

The protein microarray utilized in the present study includes 11 known 14-3-3-binding proteins, such as PCTAIRE protein kinase 1 (PCTK1) (Graeser et al., 2002), protein kinase C zeta (PRKCZ) (van der Hoeven et al., 2000), keratin 18 (KRT18) (Ku et al., 1998), myosin light polypeptide kinase (MYLK) (Haydon et al., 2002), v-abl Abelson murine leukemia viral oncogene homolog 1 (ABL1) (Yoshida et al., 2005), v-akt murine thymoma viral oncogene homolog 1 (AKT1) (Powell et al., 2002), epidermal growth factor receptor (EGFR) (Oksvold et al., 2004), cell division cycle 2 (CDC2) (Chan et al., 1999), mitogen-activated protein kinase kinase kinase 1 (MAP3K1) (Fanger et al., 1998), mitogen-activated protein kinase-activated protein kinase 2 (MAPKAPK2) (Powell et al., 2003), and stratifin (SFN) (Benzinger et al., 2005) (Table 3). All of these were not identified as a 14-3-3-binding protein in the present study. Therefore, the possibility could not be excluded that some 14-3-3 binding partners were not detected due to imperfect phosphorylation of the proteins on the array or due to 14-3-3 isoform-specific binding. Calmodulin, another known 14-3-3 interactor (Luk et al., 1999), was included as a negative control on the array and identified as negative in the present study, because the calcium-dependent interaction between 14-3-3 and calmodulin could not be detected under the calcium-free conditions we employed.

Table 3
Eleven known 14-3-3-binding proteins immobilized on the protein microarray utilized in the present study

Gene name	Database ID	Reference
PCTAIRE protein kinase 1 (PCTK1), transcript variant 3	NM_033019	Graeser et al. (2002)
Protein kinase C, zeta (PRKCZ)	NM_002744	van der Hoeven et al. (2000)
Keratin 18 (KRT18), transcript variant 1	NM_000224	Ku et al. (1998)
Myosin, light polypeptide kinase (MYLK), transcript variant 6	NM_005965	Haydon et al. (2002)
V-abl Abelson murine leukemia viral oncogene homolog 1 (ABL1), transcript variant a	NM_005157	Yoshida et al. (2005)
V-akt murine thymoma viral oncogene homolog 1 (AKT1), transcript variant 1	NM_005163	Powell et al. (2002)
Epidermal growth factor receptor (EGFR), transcript variant 1	NM_005228	Oksvold et al. (2004)
Cell division cycle 2 (CDC2), transcript variant 1	NM_001786	Chan et al. (1999)
Mitogen-activated protein kinase kinase kinase 1 (MAP3K1)	XM_042066	Fanger et al. (1998)
Mitogen-activated protein kinase-activated protein kinase 2 (MAPKAPK2), transcript variant 1	NM_004759	Powell et al. (2003)
14-3-3 Sigma, stratifin (SFN)	NM_006142	Benzinger et al. (2005)

The known 14-3-3-binding proteins, which were spotted on the protein microarray but were not detected in the present study are listed. The 14-3-3-binding proteins validated by definitive evidence are selected and shown with references.

Increasing studies indicate that 14-3-3-binding phosphorylation sites do not exactly fit the consensus motif (Aitken et al., 2002; Ku et al., 1998) and a second site is required to enhance a stable 14-3-3-target interaction (MacKintosh, 2004), and show that the 14-3-3 protein interacts with a set of target proteins in a phosphorylation-independent manner (Dai and Murakami, 2003; Henriksson et al., 2002; Zhai et al., 2001). Supporting the latter possibility, the present observations showed that the interaction of 14-3-3 with target proteins is independent of serine/threonine-phosphorylation of the binding sites of EAP30, DDX54, and STAC. This suggests that substantial numbers of 14-3-3 binding partners identified by protein microarray analysis, if not all, employ phosphorylation-independent binding domains.

All the procedure required for microarray analysis takes approximately 5 h. This analysis identified a set of 20 human proteins as 14-3-3 interactors, most of which were previously unreported except for glutathione *S*-transferase M3 (GSTM3) that was found as one of binding partners by 14-3-3 affinity purification of HeLa cell protein extracts (Pozuelo Rubio et al., 2004). Unexpectedly, the highly stringent 14-3-3-binding consensus motif was identified only in two, such as STAC and HNPRC, by the Scansite Motif Scanner search, while 15 of 20 proteins have one or several motifs when a query with the medium or low stringency was performed (Table 2). The specific binding to 14-3-3 of EAP30, DDX54, and STAC was verified by immunoprecipitation analysis of the recombinant proteins expressed in HEK293 cells. These results indicate that protein microarray is a powerful tool for rapid identification of protein–protein interactions, including those unpredicted by the Database search.

Among the 14-3-3-binding partners we identified, several proteins could be categorized as a component of multimolecular complexes involved in transcriptional regulation. ELL is a human oncogene encoding a RNA polymerase II (Pol II) transcription factor that promotes transcription elongation (Schmidt et al., 1999). EAP30 is a 30-kDa component of the ELL complex where EAP30 confers derepression of transcription by Pol II (Schmidt et al., 1999). A recent study showed that EAP30 could interact with the tumor susceptibility gene TSG101 product, a cellular factor that plays a key role in packaging of HIV virions (von Schwedler et al., 2003). DDX54 is a 97-kDa RNA helicase (DP97) that interacts with estrogen receptor (ER) and represses the transcription of ER-regulated genes (Rajendran et al., 2003). A recent study by using chromatin immunoprecipitation (ChIP) assay combined with promoter microarray analysis showed that hepatocyte nuclear factor 4-alpha (HNF4α), a master regulator of hepatocyte gene expression, interacts with the DDX54 gene promoter, together with Pol II (Odom et al., 2004). HNPRC is a member of heterogeneous nuclear ribonucleoproteins (hnRNPs) involved in pre-mRNA processing, mRNA metabolism and transport (Nakagawa et al., 1986). Increasing evidence indicates that the 14-3-3 protein and its targets are widely distributed in various subcellular compartments, including the nucleus (Dougherty and Morrison, 2004; Meek et al., 2004).

STAC is a 47-kDa cytosolic protein that has a cysteine-rich domain (CRD) of the protein kinase C family in the N-terminal half (NTF), and a src homology three (SH3) domain in the C-terminal half (CTF), suggesting its function as an adapter on which divergent signaling pathways converge (Hardy et al., 2005; Suzuki et al., 1996). STAC is expressed predominantly in the brain with the distribution in a defined population of neurons (Suzuki et al., 1996). IP analysis of mutant and truncated forms argued against an active involvement of the most stringent motif RYYSSP (*pS*172) of STAC in its binding to 14-3-3. The present observations indicated that the 14-3-3-interacting domain is located in the N-terminal segment spanning amino acid residues 2-105 of STAC and the interaction is serine/threonine phosphorylation-independent.

In conclusion, protein microarray is a useful tool for rapid and comprehensive profiling of 14-3-3-binding proteins, although the validation of the results by different methods is highly important.

Acknowledgements

This work was supported by grants from Research on Psychiatric and Neurological Diseases and Mental Health, the Ministry of Health, Labour and Welfare of Japan (H17-020), Research on Health Sciences Focusing on Drug Innovation, the Japan Health Sciences Foundation (KH21101), the Grant-in-Aid for Scientific

Research, the Ministry of Education, Science, Sports and Culture (B2-15390280 and PA007-16017320), and the Program for Promotion of Fundamental Studies in Health Sciences of the National Institute of Biomedical Innovation (NIBIO), Japan.

Appendix A. Supplementary data

Supplementary data associated with this article can be found, in the online version, at 10.1016/j.jneumeth.2005.09.015.

References

Aitken A, Baxter H, Dubois T, Clokie S, Mackie S, Mitchell K, Peden A, Zemlickova E. 14-3-3 proteins in cell regulation. Biochem Soc Trans 2002;30:351–60.

Benzinger A, Muster N, Koch HB, Yates 3rd JR, Hermeking H. Targeted proteomic analysis of 14-3-3 sigma, a p53 effector commonly silenced in cancer. Mol Cell Proteomics 2005;4:785–95.

Berg D, Holzmann C, Riess O. 14-3-3 proteins in the nervous system. Nat Rev Neurosci 2002;4:752–62.

Chan SM, Ermann J, Su L, Fathman CG, Utz PJ. Protein microarrays for multiplex analysis of signal transduction pathways. Nat Med 2004;10:1390–6.

Chan TA, Hermeking H, Lengauer C, Kinzler KW, Vogelstein B. 14-3-3σ is required to prevent mitotic catastrophe after DNA damage. Nature 1999;401:616–20.

Chen H-K, Fernandez-Funez P, Acevedo SF, Lam YC, Kaytor MD, Fernandez MH, Aitken A, Skoulakis EM, Orr HT, Botas J, Zoghbi HY. Interaction of Akt-phosphorylated ataxin-1 with 14-3-3 mediates neurodegeneration in spinocerebellar ataxia type 1. Cell 2003;113:457–68.

Culleré X, Rose P, Thathamangalam U, Chatterjee A, Mullane KP, Pallas DC, Benjamin TL, Roberts TM, Schaffhausen BS. Serine 257 phosphorylation regulates association of polyomavirus middle T antigen with 14-3-3 proteins. J Virol 1998;72:558–63.

Dai J-G, Murakami K. Constitutively and autonomously active protein kinase C associated with 14-3-3 ζ in the rodent brain. J Neurochem 2003;84:23–34.

Dougherty MK, Morrison DK. Unlocking the code of 14-3-3. J Cell Sci 2004;117:1875–84.

Fanger GR, Widmann C, Porter AC, Sather S, Johnson GL, Vaillancourt RR. 14-3-3 proteins interact with specific MEK kinases. J Biol Chem 1998;273:3476–83.

Fu H, Subramanian RR, Masters SC. 14-3-3 proteins: structure, function, and regulation. Annu Rev Pharmacol Toxicol 2000;40:617–47.

Graeser R, Gannon J, Poon RYC, Dubois T, Aitken A, Hunt T. Regulation of the CDK-related protein kinase PCTAIRE-1 and its possible role in neurite outgrowth in Neuro-2A cells. J Cell Sci 2002;115:3479–90.

Hardy K, Mansfield L, Mackay A, Benvenuti S, Ismail S, Arora P, O'Hare MJ, Jat PS. Transcriptional networks and cellular senescence in human mammary fibroblasts. Mol Biol Cell 2005;16:943–53.

Haydon CE, Watt PW, Morrice N, Knebel A, Gaestel M, Cohen P. Identification of a phosphorylation site on skeletal muscle myosin light chain kinase that becomes phosphorylated during muscle contraction. Arch Biochem Biophys 2002;397:224–31.

Henriksson ML, Francis MS, Peden A, Aili M, Stefansson K, Palmer R, Aitken A, Hallberg B. A nonphosphorylated 14-3-3 binding motif on exoenzyme S that is functional in vivo. Eur J Biochem 2002;269:4921–9.

Ichimura T, Yamamura H, Sasamoto K, Tominaga Y, Taoka M, Kakiuchi K, Shinkawa T, Takahashi N, Shimada S, Isobe T. 14-3-3 proteins modulate the expression of epithelial Na^+ channels by phosphorylation-dependent interaction with Nedd4-2 ubiquitin ligase. J Biol Chem 2005;280:13187–94.

Jin J, Smith FD, Stark C, Wells CD, Fawcett JP, Kulkarni S, Metalnikov P, O'Donnell P, Taylor P, Taylor L, Zougman A, Woodgett JR, Langeberg LK, Scott JD, Pawson T. Proteomic, functional, and domain-based analysis of in vivo 14-3-3 binding proteins involved in cytoskeletal regulation and cellular oraganization. Curr Biol 2004;14:1436–50.

Kawamoto Y, Akiguchi I, Nakamura S, Honjyo Y, Shibasaki H, Budka H. 14-3-3 proteins in Lewy bodies in Parkinson disease and diffuse Lewy body disease brains. J Neuropathol Exp Neurol 2002;61:245–53.

Ku N-O, Liao J, Omary MB. Phosphorylation of human keratin 18 serine 33 regulates binding to 14-3-3 proteins. EMBO J 1998;17:1892–906.

Layfield R, Fergusson J, Aitken A, Lowe J, Landon M, Mayer RJ. Neurofibrillary tangles of Alzheimer's disease brains contain 14-3-3 proteins. Neurosci Lett 1996;209:57–60.

Luk SCW, Ngai S-M, Tsui SKW, Fung K-P, Lee C-Y, Waye MMY. In vivo and in vitro association of 14-3-3 epsilon isoform with calmodulin: implication for signal transduction and cell proliferation. J Cell Biochem 1999;73:31–5.

MacBeath G, Schreiber SL. Printing proteins as microarrays for high-throughput function determination. Science 2000;289:1760–3.

MacKintosh C. Dynamic interactions between 14-3-3 proteins and phosphoproteins regulate diverse cellular processes. Biochem J 2004;381:329–42.

Malaspina A, Kaushik N, de Belleroche J. A 14-3-3 mRNA is up-regulated in amyotrophic lateral sclerosis spinal cord. J Neurochem 2000;75:2511–20.

Meek SEM, Lane WS, Piwnica-Worms H. Comprehensive proteomic analysis of interphase and mitotic 14-3-3-binding proteins. J Biol Chem 2004;279:32046–54.

Michaud GA, Salcius M, Zhou F, Bangham R, Bonin J, Guo H, Snyder M, Predki PF, Schweitzer BI. Analyzing antibody specificity with whole proteome microarrays. Nat Biotechnol 2003;21:1509–12.

Nakagawa TY, Swanson MS, Wold BJ, Dreyfuss G. Molecular cloning of cDNA for the nuclear ribonucleoprotein particle C proteins: a conserved gene family. Proc Natl Acad Sci USA 1986;83:2007–11.

Obenauer JC, Cantley LC, Yaffe MB. Scansite 2.0: Proteome-wide prediction of cell signaling interactions using short sequence motifs. Nucl Acids Res 2003;31:3635–41.

Odom DT, Zizlsperger N, Gordon DB, Bell GW, Rinaldi NJ, Murray HL, Volkert TL, Schreiber J, Rolfe PA, Gifford DK, Fraenkel E, Bell GI, Young RA. Control of pancreas and liver gene expression by HNF transcription factors. Science 2004;303:1378–81.

Oksvold MP, Huitfeldt HS, Langdon WY. Identification of 14-3-3ζ as an EGF receptor interacting protein. FEBS Lett 2004;569:207–10.

Pozuelo Rubio M, Geraghty KM, Wong BH, Wood NT, Campbell DG, Morrice N, Mackintosh C. 14-3-3-affinity purification of over 200 human phosphoproteins reveals new links to regulation of cellular metabolism, proliferation and trafficking. Biochem J 2004;379:395–408.

Powell DW, Rane MJ, Chen Q, Singh S, McLeish KR. Identification of 14-3-3ζ as a protein kinase B/Akt substrate. J Biol Chem 2002;277:21639–42.

Powell DW, Rane MJ, Joughin BA, Kalmukova R, Hong J-H, Tidor B, Dean WL, Pierce WM, Klein JB, Yaffe MB, McLeish KR. Proteomic identification of 14-3-3ζ as a mitogen-activated protein kinase-activated protein kinase 2 substrate: role in dimmer formation and ligand binding. Mol Cell Biol 2003;23:5376–87.

Rajendran RR, Nye AC, Frasor J, Balsara RD, Martini PG, Katzenellenbogen BS. Regulation of nuclear receptor transcriptional activity by a novel DEAD box RNA helicase (DP97). J Biol Chem 2003;278:4628–38.

Satoh J, Kuroda Y. Differential gene expression between human neurons and neuronal progenitor cells in culture: an analysis of arrayed cDNA clones in NTera2 human embryonal carcinoma cell line as a model system. J Neurosci Meth 2000;94:155–64.

Satoh J, Yamamura T. Gene expression profile following stable expression of the cellular prion protein. Cell Mol Neurobiol 2004;24:793–814.

Satoh J, Yamamura T, Arima K. The 14-3-3 protein ε isoform expressed in reactive astrocytes in demyelinating lesions of multiple sclerosis binds to vimentin and glial fibrillary acidic protein in cultured human astrocytes. Am J Pathol 2004;165:577–92.

Schmidt AE, Miller T, Schmidt SL, Shiekhattar R, Shilatifard A. Cloning and characterization of the EAP30 subunit of the ELL complex that confers derepression of transcription by RNA polymerase II. J Biol Chem 1999;274:21981–5.

Suzuki H, Kawai J, Taga C, Yaoi T, Hara A, Hirose K, Hayashizaki Y, Watanabe S. Stac, a novel neuron-specific protein with cysteine-rich and SH3 domains. Biochem Biophys Res Commun 1996;229:902–9.

Tennagels N, Hube-Magg C, Wirth A, Noelle V, Klein HW. Expression, purification, and characterization of the cytoplasmic domain of the human IGF-1 receptor using a baculovirus expression system. Biochem Biophys Res Commun 1999;260:724–8.

van der Hoeven PCJ, van der Wal JCM, Ruurs P, van Blitterswijk WJ. Protein kinase C activation by acidic proteins including 14-3-3. Biochem J 2000;347:781–5.

van Hemert MJ, Steensma HY, van Heusden GPH. 14-3-3 proteins: key regulators of cell division, signaling and apoptosis. Bioessays 2001;23:936–47.

Vidalain PO, Boxem M, Ge H, Li S, Vidal M. Increasing specificity in high-throughput yeast two-hybrid experiments. Methods 2004;32:363–70.

von Mering C, Krause R, Snel B, Cornell M, Oliver SG, Fields S, Bork P. Comparative assessment of large-scale data sets of protein–protein interactions. Nature 2002;417:399–403.

von Schwedler UK, Stuchell M, Müller B, Ward DM, Chung HY, Morita E, Wang HE, Davis T, He GP, Cimbora DM, Scott A, Kräusslich HG, Kaplan J, Morham SG, Sundquist WI. The protein network of HIV budding. Cell 2003;114:701–13.

Yoshida K, Yamaguchi T, Natsume T, Kufe D, Miki Y. JNK phosphorylation of 14-3-3 proteins regulates nuclear targeting of c-Abl in the apoptotic response to DNA damage. Nat Cell Biol 2005;7:278–85.

Zerr I, Bodemer M, Gefeller O, Otto M, Poser S, Wiltfang J, Windl O, Kretzschmar HA, Weber T. Detection of 14-3-3 protein in the cerebrospinal fluid supports the diagnosis of Creutzfeldt–Jakob disease. Ann Neurol 1998;43:32–40.

Zhai J, Lin H, Shamim M, Schlaepfer WW, Cañete-Soler R. Identification of a novel interaction of 14-3-3 with p190RhoGEF. J Biol Chem 2001;276:41318–24.

Zhang LV, Wong SL, King OD, Roth FP. Predicting co-complexed protein pairs using genomic and proteomic data integration. BMC Bioinformat 2004;5:38–52.

Zhu H, Bilgin M, Bangham R, Hall D, Casamayor A, Bertone P, Lan N, Jansen R, Bidlingmaier S, Houfek T, Mitchell T, Miller P, Dean RA, Gerstein M, Snyder M. Global analysis of protein activities using proteome chips. Science 2001;293:2101–5.

ELSEVIER

Journal of Neuroimmunology 174 (2006) 108 – 118

Journal of
Neuroimmunology

www.elsevier.com/locate/jneuroim

T cell gene expression profiling identifies distinct subgroups of Japanese multiple sclerosis patients

Jun-ichi Satoh [a], Megumi Nakanishi [a], Fumiko Koike [a], Hiroyuki Onoue [a], Toshimasa Aranami [a], Toshiyuki Yamamoto [b], Mitsuru Kawai [b], Seiji Kikuchi [c], Kyouichi Nomura [d], Kazumasa Yokoyama [e], Kohei Ota [f], Toshiro Saito [g], Masayuki Ohta [g], Sachiko Miyake [a], Takashi Kanda [h], Toshiyuki Fukazawa [i], Takashi Yamamura [a,*]

[a] *Department of Immunology, National Institute of Neuroscience, NCNP, 4-1-1 Ogawahigashi, Kodaira, Tokyo 187-8502, Japan*
[b] *National Center Hospital for Mental, Nervous and Muscular Disorders, NCNP, Tokyo 187-8502, Japan*
[c] *Department of Neurology, Hokkaido University Graduate School of Medicine, Sapporo 060-8638, Japan*
[d] *Department of Neurology, Saitama Medical School, Saitama 350-0495, Japan*
[e] *Department of Neurology, Juntendo University School of Medicine, Tokyo 113-841, Japan*
[f] *Department of Neurology, Tokyo Women's Medical University, Tokyo 162-8666, Japan*
[g] *Life Science Group, Hitachi Ltd., Saitama 350-1165, Japan*
[h] *Department of Neurology, Tokyo Medical and Dental University, Tokyo 113-8519, Japan*
[i] *Hokuyukai Neurology Hospital, Sapporo 063-0802, Japan*

Received 29 November 2005; received in revised form 30 January 2006; accepted 3 February 2006

Abstract

To clarify the molecular background underlying the heterogeneity of multiple sclerosis (MS), we characterized the gene expression profile of peripheral blood $CD3^+$ T cells isolated from MS and healthy control (CN) subjects by using a cDNA microarray. Among 1258 cDNAs on the array, 286 genes were expressed differentially between 72 untreated Japanese MS patients and 22 age- and sex-matched CN subjects. When this set was used as a discriminator for hierarchical clustering analysis, it identified four distinct subgroups of MS patients and five gene clusters differentially expressed among the subgroups. One of these gene clusters was overexpressed in MS versus CN, and particularly enhanced in the clinically most active subgroup of MS. After 46 of the MS patients were treated with interferon-beta (IFNβ-1b) for two years, IFNβ responders were clustered in two of the four MS subgroups. Furthermore, the IFNβ responders differed from nonresponders in the kinetics of IFN-responsive genes at 3 and 6 months after starting IFNβ treatment. These results suggest that T-cell gene expression profiling is valuable to identify distinct subgroups of MS associated with differential disease activity and therapeutic response to IFNβ.

Keywords: Gene expression profile; Hierarchical clustering analysis; IFNβ responder; Microarray; Multiple sclerosis; T cells

1. Introduction

Multiple sclerosis (MS) is an inflammatory demyelinating disease of the central nervous system (CNS) white matter mediated by an autoimmune process whose development is triggered by a complex interplay of both genetic and environmental factors (Compston and Coles, 2002). Intravenous administration of interferon-gamma (IFNγ) to MS patients in a previous clinical trial provoked acute relapses accompanied by activation of the systemic immune response, indicating a central role of proinflammatory T helper type 1 (Th1) lymphocytes in the immunopathogenesis of MS (Panitch et al., 1987). In contrast, treatment with interferon-beta (IFNβ) produced a

* Corresponding author. Tel.: +81 42 346 1723; fax: +81 42 346 1753.
E-mail address: yamamura@ncnp.go.jp (T. Yamamura).

0165-5728/$ - see front matter © 2006 Elsevier B.V. All rights reserved.
doi:10.1016/j.jneuroim.2006.02.004

beneficial effect on MS patients with a reduction of the relapse rate by approximately 30% (The IFNB Multiple Sclerosis Study Group, 1993; Jacobs et al., 1996; Saida et al., 2005). Recent studies indicated that an early initiation of IFNβ delays the conversion to clinically definite MS in the patients who experienced a first demyelinating event (Jacobs et al., 2000).

MS exhibits a great range of phenotypic variability. It is classified into relapsing–remitting MS (RRMS), secondary progressive MS (SPMS), or primary progressive MS (PPMS) with respect to the disease course, conventional MS (CMS) or opticospinal MS (OSMS) in terms of the lesion distribution (Saida et al., 2005), and IFNβ responder or nonresponder based on the therapeutic response to IFNβ (Waubant et al., 2003). MS brain lesions show a remarkable heterogeneity in the degree of inflammation, complement activation, antibody deposition, demyelination and remyelination, oligodendrocyte apoptosis, and axonal degeneration (Lucchinetti et al., 2000). These observations suggest that MS is a kind of neurological syndrome caused by different immunopathological mechanisms leading to the final common pathway that provokes inflammatory demyelination. Therefore, it is not surprising to find that individual MS patients show highly variable responses to IFNβ treatment. Currently, very little is known about the molecular background underlying clinical and pathological heterogeneity of MS.

DNA microarray technology is a novel approach that allows us to systematically monitor the expression of a large number of genes in disease-affected tissues (Staudt, 2001). This approach has discovered therapeutically relevant targets and prognostic markers for cancers (Alizadeh et al., 2000; van de Vijver et al., 2000), and has given new insights into the complexity of molecular interactions promoting the autoimmune process in MS (Steinman and Zamvil, 2003). Importantly, the comprehensive gene expression profiling of MS brain tissues and peripheral blood lymphocytes identified a battery of genes deregulated in MS, whose role has not been previously predicted in its pathogenesis (Lock et al., 2002; Graumann et al., 2003; Tajouri et al., 2003; Stürzbecher et al., 2003; Achiron et al., 2004). However, most of previous studies have focused on gene expression in heterogeneous populations of unfractionated lymphocytes and brain cells. Recently, by using microarray we showed that IFNβ treatment elevates the expression of 7 IFN-responsive genes in highly purified peripheral blood $CD3^+$ T cells of 13 Japanese RRMS patients (Koike et al., 2003). More recently, we found that the majority of differentially expressed genes in $CD3^+$ T cells between 72 untreated MS patients and 22 healthy control (CN) subjects were categorized into apoptosis signaling-related genes (Satoh et al., 2005).

To extend our previous studies, we conducted hierarchical clustering analysis of differentially expressed genes between MS and CN in peripheral blood $CD3^+$ T cells. Here we report that T-cell gene expression profiling classifies a heterogeneous population of Japanese MS into four subgroups that differ in the disease activity and therapeutic response to IFNβ, suggesting that this analysis could be applied for designing tailor-made treatment of MS.

2. Subjects and methods

2.1. The study population

The Research Group for IFNβ treatment of Japanese MS, sponsored by the Ministry of Health, Labour and Welfare of Japan, conducted the present study. It enrolled 72 clinically active Japanese MS patients, including 65 RRMS and 7 SPMS cases composed of 55 women and 17 men with the mean age of 36.1 ± 10.3 years, and 22 healthy control (CN) subjects composed of 16 women and 6 men with the mean age of 38.6 ± 12.3 years. The members of this research group (SK, KN, KY, KO, TK, TF and TY), all of who are certified neurologists, diagnosed individual cases according to the established criteria (McDonald et al., 2001), and followed up the patients for at least two years after entry. The patients showed the mean Expanded Disability Status Scale (EDSS) score of 2.8 ± 2.0 upon entry. No patients had a history of treatment with interferons, glatiramer acetate or mitoxantrone before enrollment, or received corticosteroids and other immunosuppressants during at least one month before blood sampling. MS patients were divided into two groups according to their own determination upon entry: one treated with IFNβ and the other without IFNβ. The IFNβ-treated group included 46 patients who started to receive an administration of 8 million units of IFNβ-1b (Betaferon, Schering, Osaka, Japan) for two years given subcutaneously on alternate days, while the IFNβ-untreated group included 26 patients who were followed up without IFNβ treatment for successive two years. From the IFNβ-treated group, blood samples were taken at three time points: before starting IFNβ treatment (designated Pre) and at 3 and 6 months after starting the treatment. In the IFNβ-untreated group, they were collected twice: at enrollment and at 6 months after the enrollment. In case of acute relapse, the patients in both groups were given intravenous methylprednisolone pulse (IVMP) following the standard protocol, although none received glatiramer acetate, mitoxantrone, or other immunosuppressants. The samples obtained during clinically obvious relapses or episodes of infection were omitted. Written informed consent was obtained from all the subjects. The present study was approved by the Ethics Committee of National Center of Neurology and Psychiatry (NCNP).

2.2. IFN β responder/nonresponder score

To evaluate the therapeutic response to IFNβ, we monitored the following six parameters during four years spanning two years before and after initiation of IFNβ

treatment; the number of clinical relapse, the day of IVMP treatment, the day of hospitalization, EDSS score, the number of lesions on T2-weighted MRI, and the patient's satisfaction on the treatment (Table 1). When compared before and after IFNβ treatment, these parameters have given three ranks and scores; good (+1), intermediate (0), and poor (−1). The total score was calculated for each patient, ranging from the maximum value of +6 to the minimum value of −6. The patients with the total score equal to or greater than +3 were considered as being the responder (R), the score from 0 to +2 as one with the undetermined response (UD), and the score equal to or smaller than −1 as the nonresponder (NR) (Table 1).

2.3. cDNA microarray analysis

The present study utilized a custom microarray containing duplicate spots of 1258 cDNA immobilized on a poly-L-lysine-coated slide glass. They were composed of well annotated genes of various functional classes, including cytokines/growth factors and their receptors, apoptosis regulators, oncogenes, transcription factors, signal transducers, cell cycle regulators and housekeeping genes (Hitachi Life Science, Kawagoe, Saitama, Japan; http://www.hitachi.co.jp/LS). Peripheral blood mononuclear cells (PBMC) were isolated from 30 ml of heparinized blood by centrifugation on a Ficoll density gradient. They were labeled with anti-CD3 antibody-coated magnetic microbeads (#130-050-101, Miltenyi Biotec, Auburn, CA), and $CD3^+$ T cells were separated by AutoMACS (Miltenyi Biotec). The remaining cells after the positive selection of $CD3^+$ T cells were harvested as $CD3^-$ non-T cell fraction as described previously (Koike et al., 2003; Satoh et al., 2005). Total RNA was isolated from the cells by using RNeasy Mini Kit (Qiagen, Valencia, CA). Five micrograms of purified RNA was in vitro amplified, and the antisense RNA (aRNA) of MS patients and CN subjects was labeled with a fluorescent dye Cy5, while pooled aRNA of three independent healthy volunteers who were not included in the present study was labeled with Cy3 for a universal reference to standardize the gene expression levels throughout the experiments. The arrays were hybridized at 62 °C for 10 h in the hybridization buffer containing equal amounts of Cy3- or Cy5-labeled cDNA, and they were then scanned by the ScanArray 5000 scanner (GSI Lumonics, Boston, MA). The data were analyzed by using the QuantArray software (GSI Lumonics). The average of fluorescence intensities (FI) of duplicate spots was obtained after global normalization between Cy3 and Cy5 signals. The gene expression level (GEL) was calculated according to the formula: GEL=FI (Cy5) of the sample/FI (Cy3) of the universal reference.

2.4. Hierarchical clustering analysis, principal component analysis, and statistical analysis

The genes whose expression was significantly different between MS and CN groups were identified by using *pierre* of the "R" statistical software system (www.cran.r-project.org) based on a Bayesian framework for analysis of microarray expression data (Baldi and Long, 2001). The error rate of this test smaller than 0.25 following the Bonferroni correction was considered as significant. Hierarchical clustering analysis and principal component analysis (PCA) were performed on a set of 286 genes differentially expressed between MS and CN groups, which were selected

Table 1
IFNβ responder/nonresponder score

Category	The parameters	Rank and score of the therapeutic response		
		Poor	Intermediate	Good
#1	Number of relapse after 2 years/number of relapse before 2 years	≧1.5	1.5–0.5	≦0.5
	Score	(−1)	0	(+1)
#2	Number of IVMP treatment after 2 years/number of IVMP treatment before 2 years	≧1.5	1.5–0.5	≦0.5
	Score	(−1)	0	(+1)
#3	Day of hospitalization after 2 years/day of hospitalization before 2 years	≧1.5	1.5–0.5	≦0.5
	Score	(−1)	0	(+1)
#4	EDSS score before treatment-EDSS score in 2 years after treatment	≦ −0.5	0.5–(−0.5)	≧0.5
	Score	(−1)	0	(+1)
#5	Number of lesions on T2-weighted MRI in 2 years after treatment/number of lesions on T2-weighted MRI before treatment	≧1.2	1.2–0.8	≦0.8
	Score	(−1)	0	(+1)
#6	Patient's satisfaction	Unsatisfied	Neither satisfied nor unsatisfied	Satisfied
	Score	(−1)	0	(+1)

The total responder/nonresponder score of six categories ranges from the maximum value of +6 to the minimum value of −6. The patients with the score equal to +3 or greater than +3 were classified as responder (R), the score ranging from 0 to +2 as undetermined (UD), and the score equal to −1 or smaller than −1 as nonresponder (NR). Abbreviations: IVMP, intravenous methylprednisolone pulse.

as a discriminator for a standard × standard algorithm on GeneSpring 7.2 (Agilent Technologies, Palo Alto, CA). The differences in clinical parameters among MS subgroups were evaluated by multiple comparison test following the Bonferroni correction.

3. Results

3.1. Microarray analysis identified 286 genes differentially expressed in peripheral blood T cells between MS and control subjects

Among 1258 genes on the microarray, 286 genes were expressed differentially in peripheral blood $CD3^+$ T cells between 72 untreated MS patients and 22 CN subjects. Among them, 78 genes were upregulated, while 208 genes downregulated in MS versus CN (Supplementary Table 1 online for all datasets). We also conducted the microarray analysis of $CD3^-$ non-T cells, composed of B cells, monocytes/macrophages and NK cells, and found that 96 genes were differentially expressed in the non-T cell fraction between MS and CN (data not shown).

3.2. Hierarchical clustering analysis identified four distinct subgroups of MS and five gene classes

Hierarchical clustering analysis was performed on $CD3^+$ T-cell samples of 72 untreated MS patients and 22 CN subjects, by using the set of 286 differentially expressed genes described above as a discriminator. This unsupervised approach, which arranged the genes and samples with a similar expression pattern to make a cluster in the dendrogram, identified four distinct

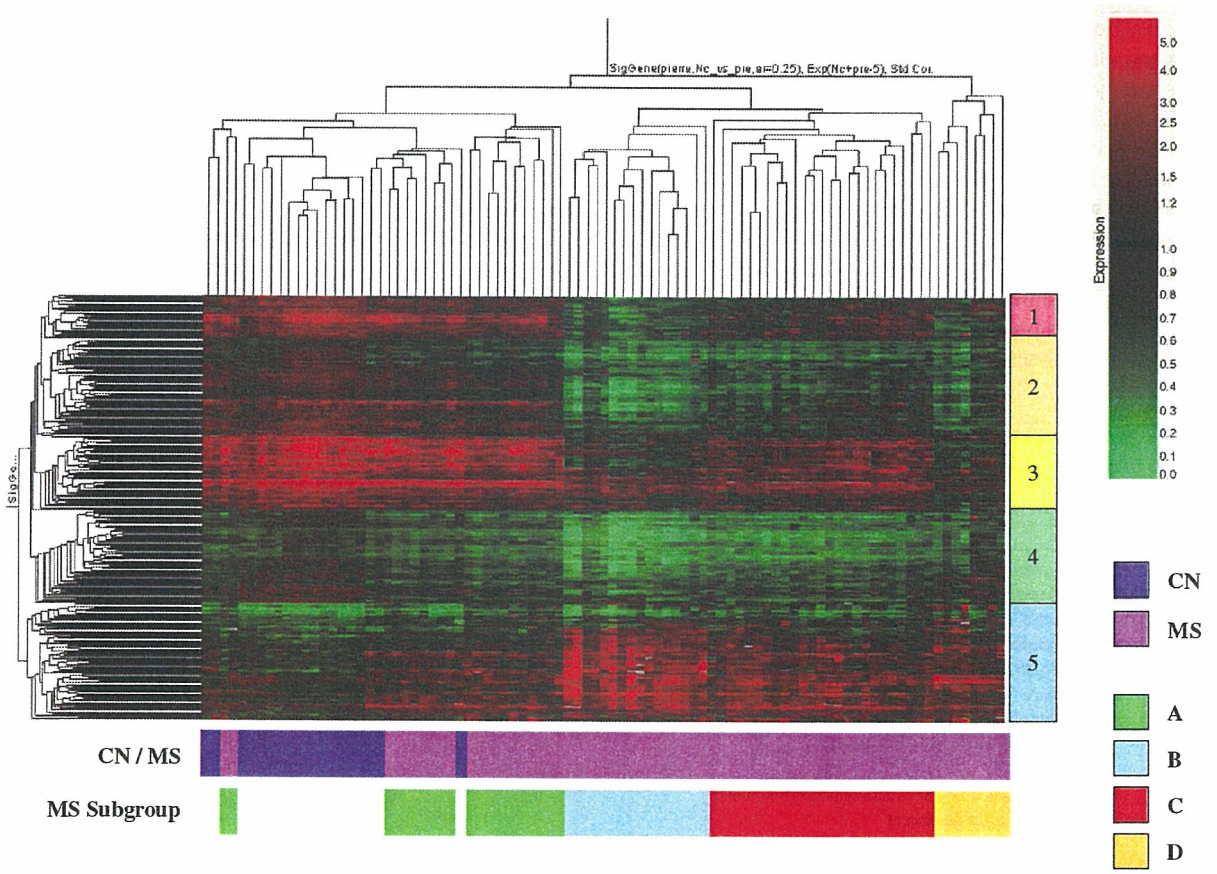

Fig. 1. Hierarchical clustering analysis of 286 genes differentially expressed between untreated MS patients and control subjects. The gene expression profile of peripheral blood $CD3^+$ T cells was studied in 72 untreated MS patients and 22 age- and sex-matched healthy control (CN) subjects, by using a 1258 cDNA microarray. Hierarchical clustering analysis was performed by selecting a set of 286 genes differentially expressed between MS and CN as a discriminator. The results are expressed in a matrix format, with each row representing the gene expression level (GEL) of a single gene in all the subjects and each column representing GEL of 286 genes in an individual subject. The matrix is shown by a pseudo-color, with red expressing upregulation, green expressing downregulation, and the color intensity representing the magnitude of the deviation from GEL 1.0 as shown on the upper right. Hierarchical clustering analysis separated MS (purple) from CN (dark blue), and classified the former into four subgroups named A (green), B (light blue), C (red) and D (yellow). The 286 genes were categorized into five classes numbered #1 (pink) to #5 (light blue).

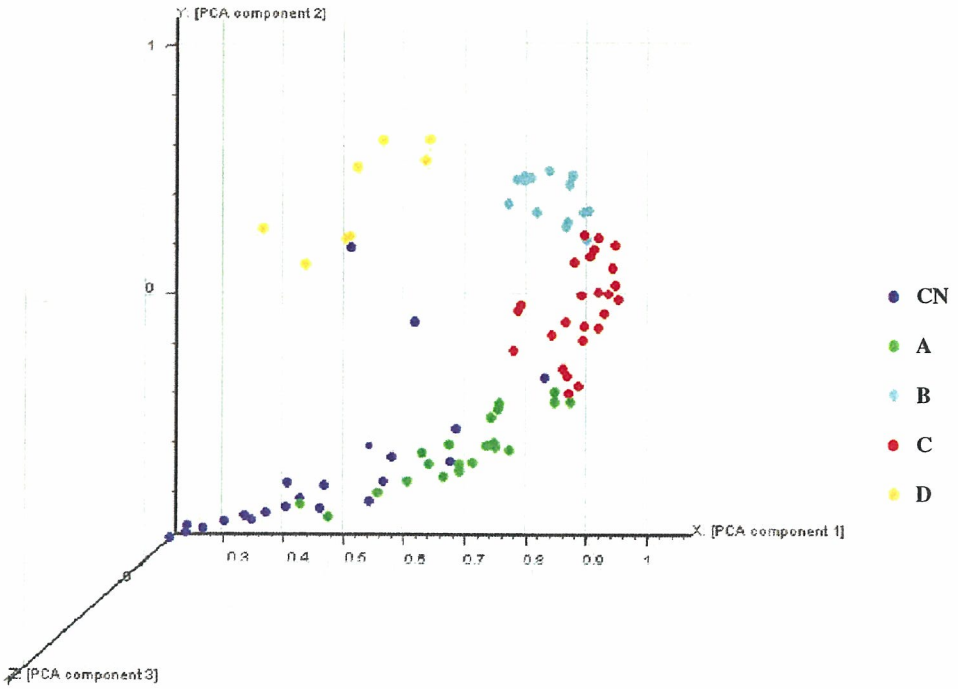

Fig. 2. Principal component analysis of 286 discriminator genes. Principal component analysis (PCA), which reduces all of the variance in the original dataset to three dimensions accounting for a significant fraction of the variance, verified a clear separation of the CN group (dark blue) and four MS subgroups named A (green), B (light blue), C (red) and D (yellow) identified by hierarchical clustering analysis.

subgroups of MS, clearly separated from the CN group (Fig. 1). We operationally designated each subgroup of MS as A, B, C and D, following the relative location in the dendrogram (Fig. 1). Principal component analysis (PCA) verified a clear discrimination of four MS subgroups and CN group (Fig. 2). Among 94 subjects examined, two MS patients and three CN subjects were considered as being unclassifiable (UC). In contrast, the clustering analysis of $CD3^-$ non-T cells did not clearly separate MS subgroups from CN (data not shown). Hierarchical clustering analysis categorized 281 of 286 differentially expressed genes into five distinct classes numbered #1 to #5 (Fig. 1 and Supplementary Table 1 online for all datasets). The remaining five, including TOP1, CHST4, SLC35A1, ST1B2, and TAF2H, were unable to be categorized into any classes. All the class #5 genes were upregulated in MS, whereas the genes of classes #1 to #4 were downregulated in MS, when compared with CN (Fig. 1). Upregulation of several class #5 genes in MS was validated by quantitative real-time RT-PCR analysis (data not shown).

3.3. Association of MS subgroups with gene clusters

Expression of the class #5 genes were elevated in all MS subgroups, whereas the classes #1 to #4 genes were downregulated in all of them, although the present study could not identify the marker genes specific for each MS subgroup. The subgroup A showed the gene expression pattern that is the most similar to CN. The similarity was supported by a partial overlap between A and CN in PCA (Fig. 2), and by the observations that one CN subject was incorporated in A, while two MS patients of A were included in CN (Fig. 1). Notably, the subgroup B showed the greatest upregulation of class #5 genes and the most prominent suppression of classes #1 to #4 genes (Fig. 1).

The class #5 genes ($n=78$) contain nine chemokines (11.5%), including CCL1, CCL3, CCL13, CCL18, CCL24, CXCL1, CXCL2, CXCL9, and CXCL14. In contrast, the classes #1 to #4 genes ($n=203$) contained only two chemokines (1.0%), such as CXCL5 and CXCL10. These observations suggest that the class #5 gene cluster is highly enriched in chemokine genes.

Fig. 3. Clinical characteristics of microarray-determined four MS subgroups. MS patients were classified into four distinct subgroups named A, B, C, and D by hierarchical clustering analysis. The bar indicates the data of individual patients. The number of relapse, the day of IVMP treatment, the day of hospitalization, and the number of lesions on T2-weighted MRI represent the data of 2 years before enrollment. Abbreviations: EDSS, Expanded Disability Status Scale; IVMP, intravenous methylprednisolone pulse; R/NR, responder/nonresponder.

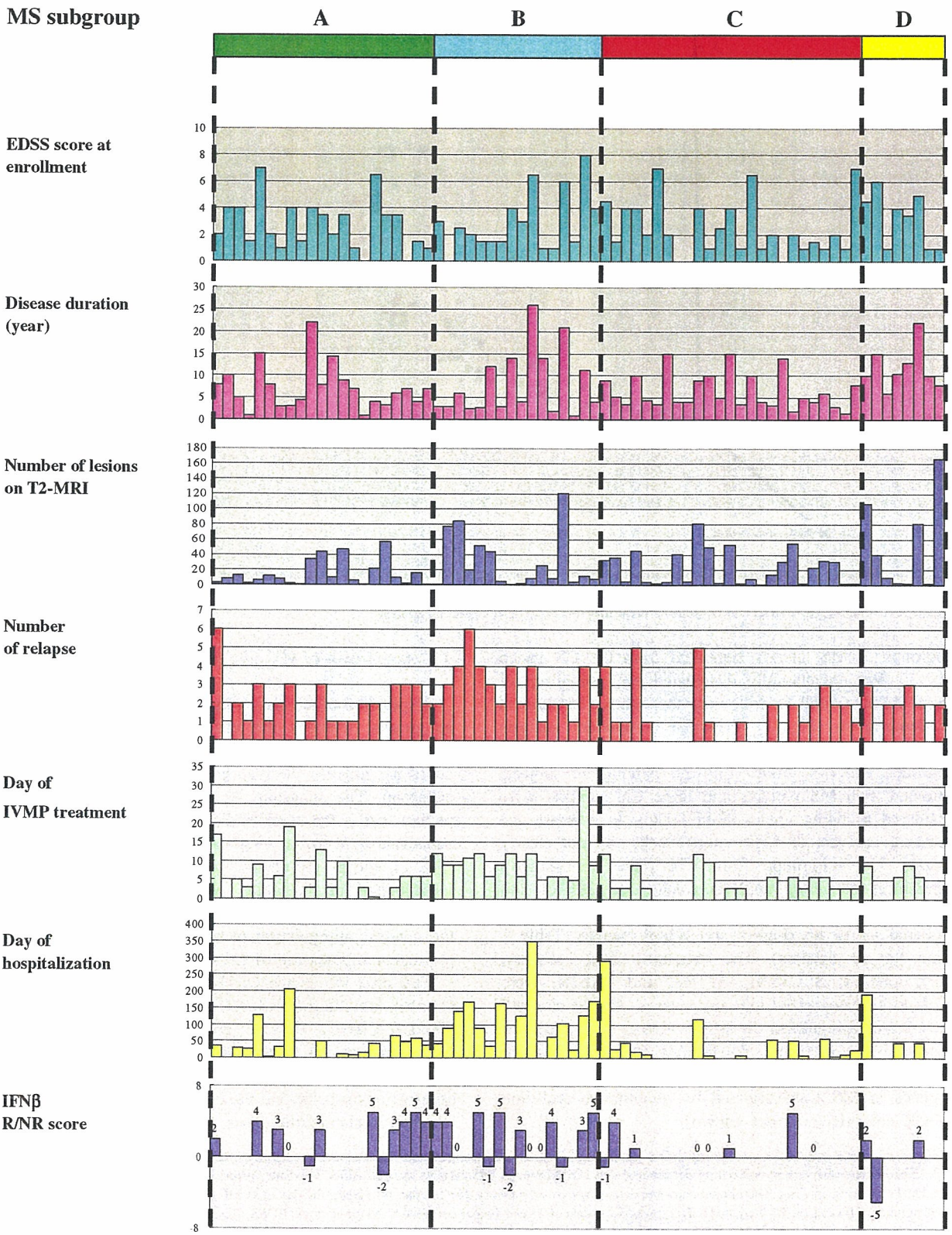
MS subgroup
A
B
C
D
EDSS score at enrollment
Disease duration (year)
Number of lesions on T2-MRI
Number of relapse
Day of IVMP treatment
Day of hospitalization
IFNβ R/NR score

Table 2
The therapeutic response to IFNβ in microarray-determined four MS subgroups

	Total	A	B	C	D	UC
IFNβ-treated patients (*n*)	46	14	14	11	5	2
Age of IFNβ-treated patients (average, SD)	34.9±9.2	33.2±7.6	36.5±10.4	33.1±8.3	36.2±13.3	41.5
Male to female ratio of IFNβ-treated patients	8 to 38	1 to 13	3 to 11	3 to 8	0 to 5	1 to 1
IFNβ responder/nonresponder score (average, SD)	1.9±2.6	2.5±2.3	2.1±2.6	1.3±2.1	−0.3±4.0	3
Dropout during a follow-up (*n*)	7	2	0	3	2	0
IFNβ responder (*n*, %)	19 (41.3%)	8 (57.1%)	8 (57.1%)	2 (18.2%)	0 (0%)	1 (50%)
IFNβ nonresponder (*n*)	7	2	3	1	1	0
Undetermined group (*n*)	13	2	3	5	2	1
The patients with IFNβ-related adverse effects (*n*, %)	29 (63.0%)	8 (57.1%)	9 (64.3%)	7 (63.6%)	4 (80%)	1 (50%)
Increase in the number of lesions on T2-weighted MRI during a follow-up (average, SD)	1.7±9.7	−2.0±7.1	2.8±6.6	7.6±15.8	−0.7±8.1	−3.5
The patients satisfied with IFNβ treatment (*n*, %)	17 (37.0%)	8 (57.1%)	6 (42.9%)	2 (18.2%)	0 (0%)	1 (50%)
The patients neither satisfied nor unsatisfied with IFNβ treatment (*n*)	21	4	7	7	2	1
The patients unsatisfied with IFNβ treatment (*n*)	8	2	1	2	3	0

Among 72 MS patients, 46 patients were treated with IFNβ for two years after enrollment. The therapeutic response was evaluated by IFNβ responder/nonresponder score shown in Table 1. Abbreviations: UC, unclassifiable.

3.4. Clinical characteristics of microarray-determined MS subgroups

Next, we investigated clinical characteristics of four MS subgroups (Supplementary Table 2 online and Fig. 3). No statistically significant differences were found among the subgroups in the age, disease duration, EDSS score, and the number of lesions on T2-weighted MRI at enrollment. However, there was a trend that the subgroup D showed a greater EDSS score and had a larger number of MRI lesions, suggestive of an advanced stage of the disease (Supplementary Table 2 online). The female outnumbered the male in all the subgroups. The male to female ratio was relatively higher in C, while no male patient was included in D. The patients with RRMS outnumbered those with SPMS in all the subgroups, although there was a mild bias for SPMS in B. The number of relapse, the day of IVMP treatment, and the day of hospitalization during preceding two years before enrollment were the largest and longest in subgroup B, and this difference was statistically significant, when compared between subgroups B and C ($p=0.0128$, 0.0183, and 0.0329 for each parameter) (Supplementary Table 2 online and Fig. 3). These observations indicate that the subgroup B included the patients who were the clinically most active before starting IFNβ.

In all MS subgroups, the conventional form of MS (CMS) greatly outnumbered non-CMS, the latter was composed of the opticospinal form (OSMS) and multifocal recurrent myelitis without optic nerve involvement. No obvious association was identified between a particular MS subgroup and the spinal cord involvement. However, 5 of 6 patients having the lesions restricted to the cerebrum (CBR) were included in subgroup C (Supplementary Table 2 online). These observations suggest that the status of T-cell gene expression might affect the lesion distribution in this subgroup.

3.5. IFN β responders were clustered in subgroups A and B

Based on the patient's own determination at enrollment, 72 MS patients were separated into two groups; 46 who started to receive IFNβ treatment for following two years, and 26 who were followed up without IFNβ treatment for successive two years (Supplementary Table 3 online). All the IFNβ-treated patients were evaluated by the IFNβ responder/nonresponder score (Table 1) at the end of the two year-treatment. They were classified into 19 IFNβ responders, 7 nonresponders, 13 undetermined subjects, and 7 dropouts (Table 2). The difference in the score among the subgroups (A: 2.5±2.3; B: 2.1±2.6; C: 1.3±2.1; and D: −0.3±4.3) did not reach the level of statistical significance (Table 2). However, there existed a trend that IFNβ responders were clustered either in subgroup A or B. Because the subgroup A contains the greatest proportion of IFNβ responders (57.1%), the patients of A were judged as being the most IFNβ responsive (Table 2). All the responders of A expressed a satisfaction on IFNβ treatment. The patients of the subgroup B also showed a good response equivalent to A (57.1%), although the number of satisfied patients was smaller. In contrast, only 2 of 11 IFNβ-treated patients in subgroup C (18.2%) and none of the patients in subgroup D were judged as IFNβ responders. The patients of C showed a trend for great increase in the number of MRI lesions during IFNβ treatment, consistent with the poor response to IFNβ (Table 2). A battery of IFNβ treatment-related adverse effects, including skin reactions, flu-like symptoms, leukocytopenia, depression, and amenorrhea, were observed in more than 50% of IFNβ-treated patients in all the subgroups (Table 2). Seven patients of the IFNβ-treated group discontinued the treatment: five due to adverse effects, one due to a severe relapse, and another by a personal reason.

We also studied T-cell gene expression profile of IFNβ-treated MS patients at 3 or 6 months after starting the

treatment. Although hierarchical clustering analysis classified these patients into several subgroups, they did not match with the subgroup A, B, C, or D determined at pretreatment (data not shown). Furthermore, no significant association was identified between these new clusters and the response to IFNβ. These observations suggest that T-cell gene expression profiling at pretreatment is the most valuable to predict the clinical outcome, whereas the analysis after starting IFNβ treatment is less informative.

3.6. Temporal profile of IFN-responsive gene expression in the first six months discriminated responders and nonresponders

Finally, we investigated the temporal expression profile of the genes with IFN-responsive promoter elements named IFN-responsive genes (IRGs) following IFNβ treatment. As we previously reported (Koike et al., 2003), IFNβ treatment for 6 months enhanced the expression of a battery of IRGs in T cells (Fig. 4). A remarkable difference was found between IFNβ responders (R) and nonresponders (NR) in the kinetics of several IRGs, such as IFN-stimulated protein 15 (ISG15), small inducible cytokine A2 (SCYA2, CCL2, or MCP-1), TNF receptor subfamily member 1B (TNFRSF1B, TNFRp75), and IFNα-inducible protein 27 (IFI27) (Fig. 5). The IFNβ responders exhibited a pattern of persistent upregulation during 6 months of the treatment. In contrast, the nonresponders showed a seesaw pattern, i.e. higher upregulation at 3 months than the responders, followed by substantial downregulation at 6 months. The differences between R and NR in the kinetics of both TNFRSF1B and IFI27 levels from 3 to 6 months were statistically significant ($p=0.0092$ and 0.0307, respectively) (Fig. 5). These observations suggest that IFNβ nonresponders also well respond to IFNβ at 3 months, but they could not maintain the responsiveness until 6 months.

4. Discussion

To elucidate the molecular basis underlying clinicopathological variability of MS, we conducted a comprehensive study that combines T-cell gene expression profiling and clinical characteristics of Japanese MS patients. Hierarchical clustering analysis of 286 genes differentially expressed between 72 untreated MS patients and 22 CN subjects classified a clinically heterogeneous population of MS into four distinct subgroups, named A, B, C, and D, and identified five gene classes numbered #1 to #5. The class

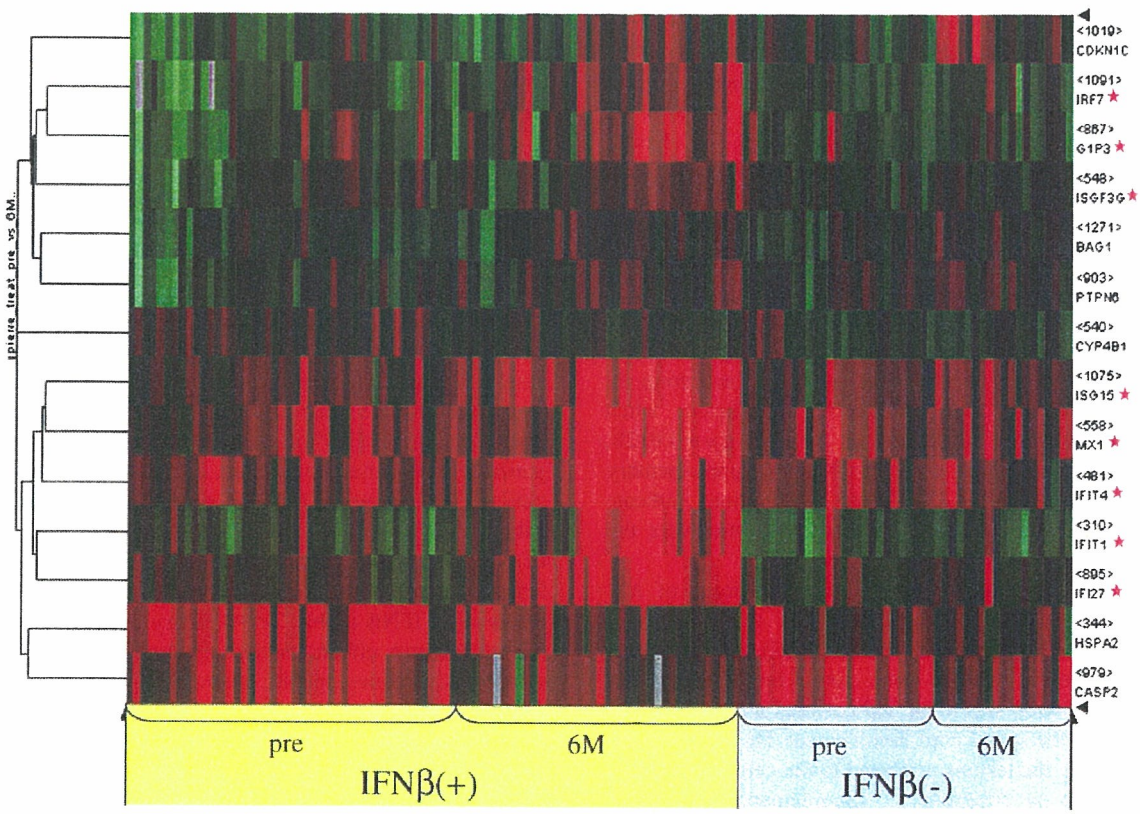

Fig. 4. Induction of IFN-responsive genes in IFNβ-treated MS patients. Seventy-two MS patients were divided into IFNβ-treated group (IFNβ+; $n=46$) and untreated group (IFNβ−; $n=26$). A cluster of known IFN-responsive genes (IRGs) indicated by the star were significantly upregulated exclusively in IFNβ-treated patients at 6 months after starting the treatment.